

Exclusive Semileptonic $b \rightarrow u\ell\nu$ Decays at CLEO

S. Stone*

Physics Department of Syracuse University
Syracuse NY, 13104, USA

Updated CLEO results are presented for branching ratios and four-momentum transfer, q^2 , dependence of exclusive charmless semileptonic B decays, where the final state hadron is either a π , ρ , ω , η or η' . These results have comparable accuracies with those of other experiments. We address the issue of flavor singlet couplings by limiting $\Gamma(B^+ \rightarrow \eta'\ell^+\nu)/\Gamma(B^+ \rightarrow \eta\ell^+\nu) > 2.5$ at 90% CL. We also extract a value of $|V_{ub}| = (4.3 \pm 0.4 \pm 0.2_{-0.4}^{+0.6}) \times 10^{-3}$ in one particular unquenched lattice QCD model using $\pi\ell^+\nu$ data above q^2 of 16 GeV².

I. INTRODUCTION

In this paper I present improved measurements of $B^0 \rightarrow \pi^-\ell^+\nu$ and $\rho^-\ell^+\nu$ branching ratios and four-momentum transfer, q^2 , dependencies. Also shown is evidence for $\mathcal{B}(B^+ \rightarrow \eta'\ell^+\nu)$ and an upper limit for $B^+ \rightarrow \eta\ell^+\nu$. These result use a “neutrino reconstruction” technique that is an extension of a previous CLEO analyses [1], based on CLEO II and II.V data. Here we include CLEO III data, representing an increase of 60% in the sample, for a total of 15.4×10^6 $B\bar{B}$ events.

Semileptonic B decays proceed when the b quark transforms to a c or u quark emitting a virtual W that manifests itself as a lepton-neutrino pair. For a B meson decaying into a single hadron (h), the decay rate can be written exactly in terms of the four-momentum transfer defined as:

$$q^2 = (p_B^\mu - p_h^\mu)^2 = m_B^2 + m_h^2 - 2E_h m_B . \quad (1)$$

For decays to light pseudoscalar hadrons, via the $b \rightarrow u$ transition, and “virtually massless” leptons, the decay width is given by:

$$\frac{d\Gamma(B \rightarrow P\ell^+\nu)}{dq^2} = \frac{|V_{ub}|^2 G_F^2 p_P^3}{24\pi^3} |f_+(q^2)| , \quad (2)$$

where p_P is the three-momentum of P in the D rest frame, and $f_+(q^2)$ is a “form-factor,” whose normalization must be calculated theoretically, although its shape can be measured, in principle.

For B decays into a vector meson final state we measure both q^2 and $\cos\theta_{WL}$, where θ_{WL} is the angle between the ℓ^+ direction in the W rest frame and the W direction in the B rest frame. The double differential decay rate then is related to the helicity amplitudes, H_i

as

$$\frac{d\Gamma(B \rightarrow V\ell^+\nu)}{dq^2 d\cos\theta_{WL}} = \quad (3)$$

$$|V_{ub}|^2 \frac{G_F^2 M_B^2 P_V q^2}{128\pi^3} \left[(1 - \cos\theta_{WL})^2 \frac{|H_+|^2}{2} \right. \\ \left. + (1 + \cos\theta_{WL})^2 \frac{|H_-|^2}{2} + \sin^2\theta_{WL} |H_0|^2 \right] .$$

II. EXPERIMENTAL METHODS

We first select events with either an e^\pm or μ^\pm with momenta greater than 1 GeV/c. Events with more than one such lepton are rejected, since multiple leptons are indicative of more than one semileptonic decay. We also require the events to be of spherical shape in momentum space, and to have a net observed charge of zero except in modes with a single pseudoscalar hadron where the requirement is loosened to ± 1 .

The technique of neutrino reconstruction makes use of the energy and momentum deposited by all found (i. e. visible) charged tracks and photons in the event. Then the neutrino four-vector is formed from the missing energy and momentum as:

$$\vec{p}_{\text{miss}} = \vec{p}_{\text{CM}} - \vec{p}_{\text{visible}} \quad (4)$$

$$E_{\text{miss}} = E_{\text{CM}} - E_{\text{visible}} .$$

The resolution in \vec{p}_{miss} is ~ 0.1 GeV/c, r.m.s. Since the missing-mass-squared

$$\text{MM}^2 = E_{\text{miss}}^2 - \vec{p}_{\text{miss}}^2, \quad (5)$$

should peak at zero, we require $\text{MM}^2/2E_{\text{miss}} < 0.5$ GeV. This requirement takes into account the scaling of the MM^2 resolution proportional to E_{miss} .

Then we look at signals in the ΔE -invariant mass plane ($M_{h\ell\nu}$), where

$$\Delta E = E_h + E_\ell + E_{\text{miss}} - E_{\text{beam}} \quad (6)$$

$$M_{h\ell\nu}^2 = E_{\text{beam}}^2 - (\vec{p}_h^2 + \vec{p}_\ell^2 + \alpha \vec{p}_{\text{miss}}^2) ;$$

here E_{miss} is replaced with $|p_{\text{miss}}|$, because the latter has better resolution, and the parameter α is adjusted for each hypothesis in order ensure that ΔE is zero.

*Electronic address: stone@physics.syr.edu

The $\pi^-\ell^+\nu$ data are analyzed in four separate bins of q^2 . For $\rho\ell^+\nu$, the models differ greatly on their $\cos\theta_{WL}$ dependencies. Fig. 1 shows the ratio of the predicted form-factors for $\cos\theta_{WL} < 0/\cos\theta_{WL} > 0$, as a function of q^2 . These differences can lead to substantial systematic errors. We reduce these by analyzing the data in two separate $\cos\theta_{WL}$ bins, one above and one below zero and four q^2 bins for a total of 8 intervals.

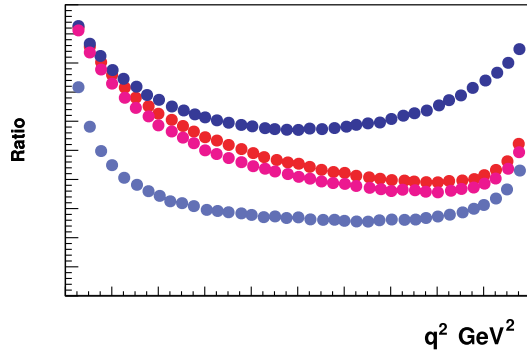


FIG. 1: Predictions of different models for the ratio of form-factors for $\cos\theta_{WL} < 0/\cos\theta_{WL} > 0$, as a function of q^2 . From top to bottom [2, 3, 4, 5].

The $\eta'\ell^+\nu$ data are split into two q^2 bins at 10 GeV^2 , while the $\eta\ell^+\nu$ sample is integrated over all q^2 .

Monte Carlo simulation of signal semileptonic events and generic $b \rightarrow c$ backgrounds in terms of the kinematic variables $M_{h\ell\nu}$ and ΔE is shown in Fig. 2. The backgrounds peak at low values of $M_{h\ell\nu}$ and ΔE , and are well separated from the signal which peaks at the B mass and ΔE of zero.

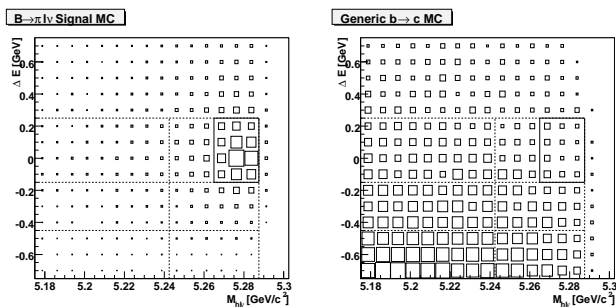


FIG. 2: Distribution of $B^0 \rightarrow \pi^-\ell^+\nu$ (left) and generic $b \rightarrow c$ events (right) in variables $M_{h\ell\nu}$ and ΔE from Monte Carlo simulation. The signal region is shown by the rectangular box.

The data are fit simultaneously for all modes in the separate bins of q^2 and $\cos\theta_{WL}$ discussed above. The projections of the fits for $\pi\ell^+\nu$, $(\rho + \omega)\ell^+\nu$ and $\eta^{(\prime)}\ell^+\nu$ are shown in Figs. 3, 4 and 5, respectively. For the η' final state only data for $q^2 < 10 \text{ GeV}^2$ is used, while the other modes are shown summed over all q^2 .

The branching fractions, integrated over q^2 are given in Table I. The $\eta'\ell^+\nu$ is observed at the 3σ level, while for

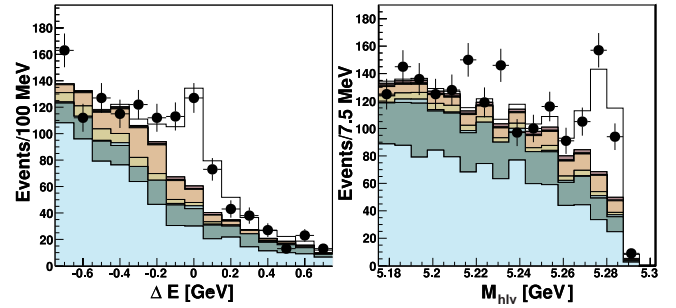


FIG. 3: Projections of the data fit for $(\pi^- + \pi^0)\ell^+\nu$, shown as points with error bars. The background components are (listed from bottom to top in different shades): $B \rightarrow X_c\ell^+\nu$, continuum, other $B \rightarrow X_u\ell^+\nu$ channels, specific $B \rightarrow (\rho + \omega)\ell^+\nu$ cross-feed, π^+ and π^0 cross-feed. The solid line shows the sum.

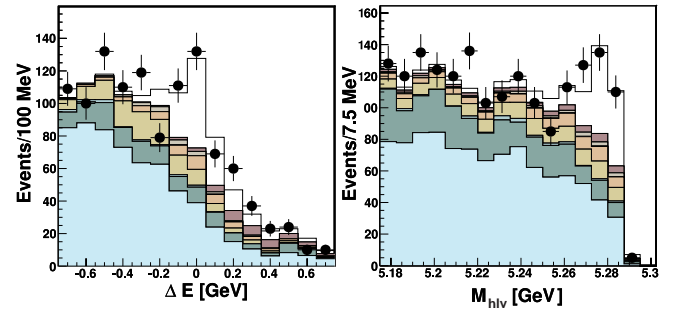


FIG. 4: Projections of the data fit for $(\rho^+ + \rho^0 + \omega)\ell^+\nu$, shown as points with error bars. The background components are the same as in Fig. 3, except that the $\rho\ell^+\nu$ background is $\pi\ell^+\nu$. The solid line shows the sum.

$\eta'\ell^+\nu$ we have a substantially smaller upper limit. Thus we can quote the ratio

$$R' \equiv \frac{\Gamma(B^+ \rightarrow \eta'\ell^+\nu)}{\Gamma(B^+ \rightarrow \eta\ell^+\nu)} > 2.5 \text{ at } 90\% \text{ CL.} \quad (7)$$

Anomalously large inclusive production of η' at high momentum has been observed in B decays [6]. Several models have attempted to explain this phenomena by an enhanced gluonic form-factor [7], or by flavor singlet coupling [8]. Measurement of inclusive η' production from the $\Upsilon(1S)$ has ruled out the form-factor explanation [9]. Our limit on R' supports an enhanced flavor singlet coupling.

The systematic errors in these measurements are dominated by the uncertainty on neutrino reconstruction, which is particular large in the η and η' modes due to shower resolution.

These branching fractions are of comparable precision to other results, some of which used much larger data samples. They have been tabulated by the Heavy Flavor Averaging Group [12].

The results for the q^2 dependence of the branching ratios are shown in Fig. 6 and compared with two theoretical predictions.

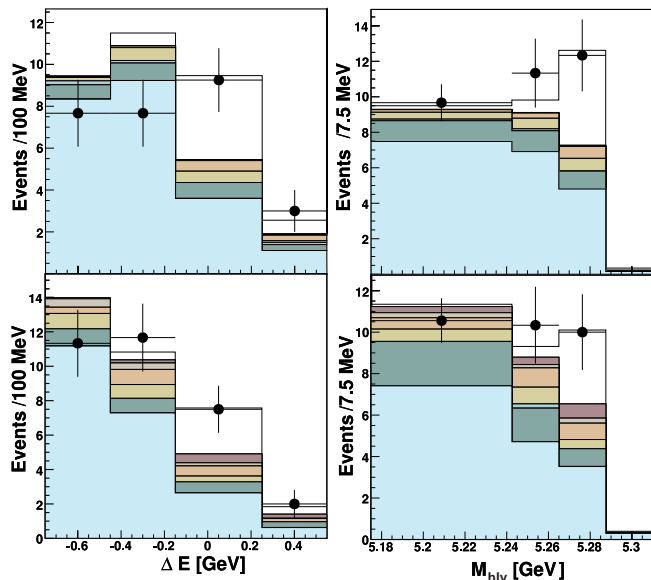


FIG. 5: The projections of the data fit for $\eta'\ell^+\nu$ (top) and $\eta\ell^+\nu$ (bottom), shown as points with error bars. The background components are the same as in Fig. 3. The solid line shows the sum.

TABLE I: Measured branching fractions. The modes with π^0 or ρ^0 and ω^0 are averaged in assuming isospin symmetry. Errors are (in order): statistical, systematic and model.

Final State	$\mathcal{B} \times 10^{-4}$
$\pi^-\ell^+\nu$	$1.37 \pm 0.15 \pm 0.12 \pm 0.01$
$\rho^-\ell^+\nu$	$2.93 \pm 0.37 \pm 0.39 \pm 0.04$
$\eta\ell^+\nu$	< 1.01 at 90% CL
$\eta'\ell^+\nu$	$2.66 \pm 0.80 \pm 0.57 \pm 0.04$

We can translate these measurements into values of $|V_{ub}|$ using theoretical models. For example, using our $B \rightarrow \pi\ell^+\nu$ rate in the $q^2 > 16 \text{ GeV}^2$ range, and the HPQCD unquenched lattice QCD calculation [10], results in

$$|V_{ub}| = (4.3 \pm 0.4 \pm 0.2_{-0.4}^{+0.6}) \times 10^{-3}, \quad (8)$$

where the last error is due to the model. This results are

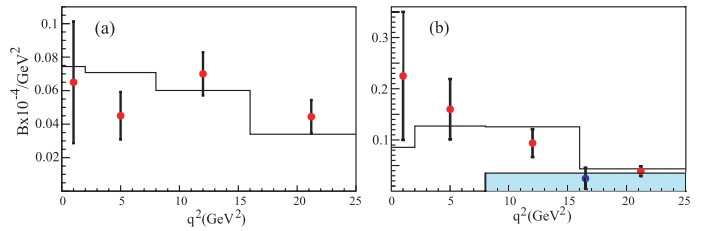


FIG. 6: Branching fractions as a function of q^2 for (a) $\pi\ell^+\nu$ and (b) $\rho\ell^+\nu$ shown as points with error bars. In (a) the solid lines indicate the HPQCD prediction [10] normalized to the data, and in (b) the model of Ball and Zwicky [3]. In (b) the shaded point is for $\cos\theta_{WL} < 0$, while the other points are for $\cos\theta_{WL} > 0$.

approximately a factor of two less precise statistically than the current b -factory results [11].

III. CONCLUSIONS

We find $\mathcal{B}(B^0 \rightarrow \pi^-\ell^+\nu) = (1.37 \pm 0.15 \pm 0.12 \pm 0.01) \times 10^{-4}$ and $\mathcal{B}(B^0 \rightarrow \rho^-\ell^+\nu) = (2.93 \pm 0.37 \pm 0.39 \pm 0.04) \times 10^{-4}$. The model dependent systematic errors have been greatly reduced by determining the partial branching ratios in bins of q^2 and $\cos\theta_{WL}$.

We extract a value of $|V_{ub}| = (4.3 \pm 0.4 \pm 0.2_{-0.4}^{+0.6}) \times 10^{-3}$ using the unquenched lattice QCD model of HPQCD with our $\pi\ell^+\nu$ data above q^2 of 16 GeV^2 .

We also show that $\eta'\ell^+\nu$ is more than 2.5 times larger than $\eta\ell^+\nu$ leading credence to an enhanced flavor singlet coupling.

Acknowledgments

I thank the U. S. National Science Foundation for support. I had useful conversations concerning this work with M. Artuso, and R. Gray.

[1] S. B. Athar *et al.* (CLEO), Phys. Rev. **D68**, 072003 (2004).
 [2] D. Melikhov and B. Stech, Phys. Rev. **D62**, 014006 (2000) [hep-ph/0001113].
 [3] P. Ball and R. Zwicky, Phys. Rev. **D71**, 014015 (2005) [hep-ph/0406232].
 [4] L. Del Debbio *et al.* (UKQCD), Phys. Lett. **B416**, 392 (1998) [hep-lat/9708008].
 [5] D. Scora and N. Isgur, Phys. Rev. **D52**, 2783 (1995). [hep-ph/0001113].
 [6] T. E. Browder *et al.* (CLEO), Phys. Rev. Lett. **81**, 1786 (1998) [hep-ex/9804018]; G. Bonvicini *et al.* (CLEO), Phys. Rev. **D68**, 011101 (2003) [hep-ex/0303009]; B. Aubert *et al.* (BABAR), Phys. Rev. Lett. **93**, 061801

(2004) [hep-ex/0401006].
 [7] See for example A. Ali and A. Y. Parkhomenko, Eur. Phys. J. **C30**, 183 (2003) [hep-ph/0304278], and references therein.
 [8] C.S. Kim, S. Oh, and C. Yu, Phys. Lett. **B590**, 223 (2004), and references therein.
 [9] O. Aquines *et al.* (CLEO), Phys. Rev. **D74**, 092006 (2006).
 [10] E. Gulez *et al.*, (HPQCD), Phys. Rev. **D73**, 074502 (2006).
 [11] W.-M. Yao *et al.*, J. Phys. **G33**, 1 (2006).
 [12] <http://www.slac.stanford.edu/xorg/hfag/semi/index.html>.